picoWear: High-datarate NFC Body Networks with Digitally-Balanced Meander E-textiles

Ryo Takahashi*, *Member, IEEE,* Yuga Kajihara*, Wakako Yukita, Tomoyuki Yokota, *Member, IEEE,* Takao Someya, *Member, IEEE,* and Yoshihiro Kawahara, *Member, IEEE*

***Abstract*—Clothing with near-field communication (NFC) coils can stably power up and efficiently communicate with battery-free devices on the skin, without body electromagnetic interference. However, such networks reach only tens of kbit/s due to its narrowband, so they serve only slow sensors. Here we show picoWear, meander-coil clothing that keeps a 1.7 Mbit/s NFC link, close to the $2\,\mathrm{Mbit/s}$ PHY rate of Bluetooth Low Energy, while the wearer moves. The two coils of picoWear form a bridge circuit that cancels the strong carrier at the receiver. When the textile wiring stretches and bends, the two coils no longer match, and the carrier leaks through. We show that shifting the phase between the two drive signals enables to restore the balance. This phase shift lowers the transmission power level needed for a bit error rate (BER) of 10^{-3} by more than 11 dB when one arm is fully bent (70% mismatch error). Simply changing the phase against the wearer's motion (motion-aware phase control) lowers the BER at matched mismatch error during free movement from 2.1×10^{-2} to 6.1×10^{-4}.**

***Index Terms*—NFC VHBR, e-textile, meander coil, body area network, impedance balance, digital bridge, knit.**

I. Introduction

THIN skin devices can now record hospital-grade body signals such as blood oxygen, pulse waves, and ultrasound images of the heart in daily life [1], [2], but to be worn all day they must run without batteries or wires. Clothing made with conductive textiles can run such devices through near-field communication (NFC) [3]–[7]. The $13.56\,\mathrm{MHz}$ field passes through the body with little loss and stays close to the textile, so the clothing can power the devices and exchange data with them without disturbing, or being disturbed by, other radios. Popular radios such as Bluetooth Low Energy (BLE) and IEEE 802.15.6 body area networks [8] reach $\mathrm{Mbit/s}$, but at $2.4\,\mathrm{GHz}$ they easily interfere with the radios of people nearby, lose power in the body, and need a battery in every device. Metamaterial textiles guide $2.4\,\mathrm{GHz}$ waves along the clothing [9], but devices on the skin side lose much of the signal in the body [10]. Body channel communication sends signals through the body, but it needs electrodes on the skin, and safety limits on the current through the body make it hard to deliver even milliwatts [11]. NFC textiles safely deliver milliwatts to watts [7], [12], [13], but they are slow. NFC allows 106–$848\,\mathrm{kbit/s}$, but its command-and-response protocol cuts the real throughput to tens of $\mathrm{kbit/s}$, so NFC clothing has served only slow sensors such as temperature and strain sensors [14]. A recent custom NFC system proposed carrier-synchronized time-division multiple access (TDMA), which shares the clothing among several tags in turn [15].

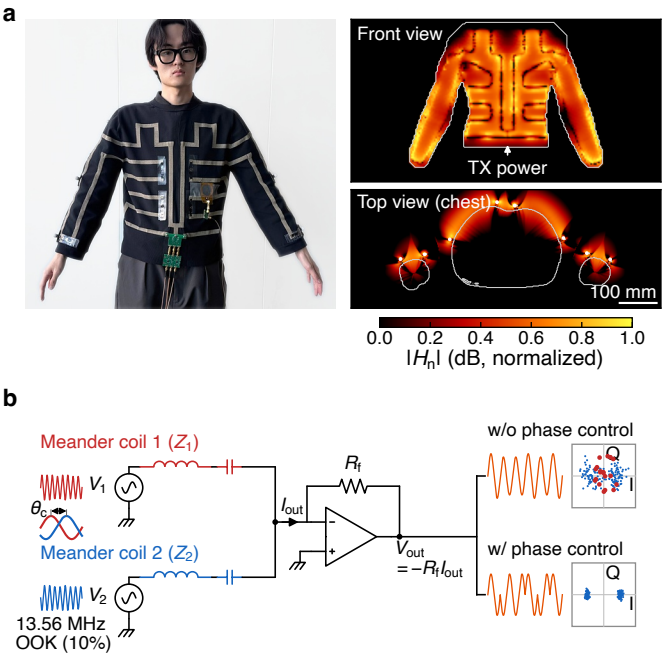


Fig. 1. (a) picoWear: meander-coil clothing, and the simulated field normal to it, $|H_\mathrm{n}|$, at $13.56\,\mathrm{MHz}$, from the front and in a cut through the chest (dots: lines; color: a $25\,\mathrm{dB}$ range scaled to 0–1). (b) Digital-bridge circuit. The two carriers drive the two meander coils, each tuned by a series capacitor, whose return currents are summed by a transimpedance amplifier with a feedback resistor R_f. Right: sketches of the output and its IQ constellation (red: bit errors), after measured ones.

Here we propose picoWear, meander-coil clothing that keeps a $1.7\,\mathrm{Mbit/s}$ NFC link while the wearer moves. It raises the rate of this TDMA to the very high bit rate (VHBR) of ISO/IEC 14443, where tags send data by binary phase-shift keying (BPSK) [16]; this rate, close to that of BLE, suits data-heavy skin devices such as electromyography (EMG) patches and skin imagers. Its coils are knitted into the clothing (Fig. 1(a)) [6], [14] and run back and forth across the body, so the fields of neighboring lines cancel away from the body but stay strong near it, and a tag anywhere along the wiring can be powered and read. Two such coils, one on each half of the body, form a twin meander coil: a bridge that cancels the carrier at the receiver. We aim to use the whole matched

This work was supported in part by JST under Grant JPMJPR2515 and Grant JPMJCS25N4, and in part by JSPS KAKENHI under Grant JP22K21343. (Corresponding author: Ryo Takahashi.)

The authors are with the Department of Electrical Engineering and Information Systems, The University of Tokyo, Tokyo 113-8656, Japan (e-mail: takahashi@akg.t.u-tokyo.ac.jp).

*R. Takahashi and Y. Kajihara contributed equally to this work.

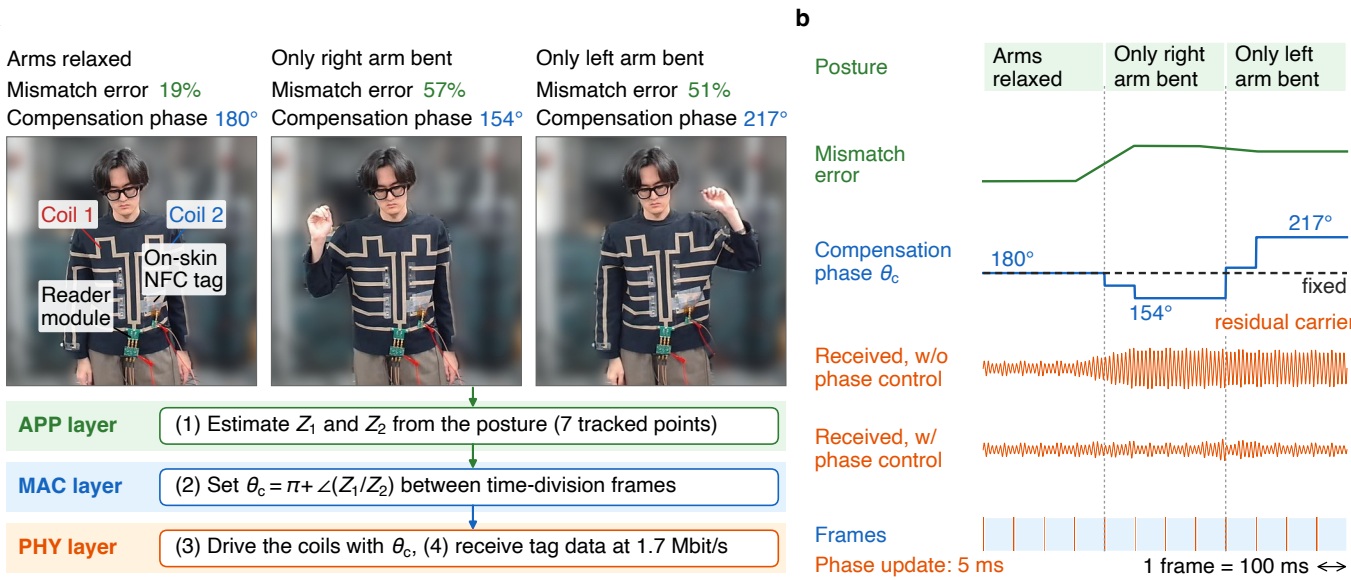


Fig. 2. (a) Top: the wearer with the arms relaxed and with only the right or only the left arm bent (camera frames, background blurred), with the mismatch error and the compensation phase θ_c set by the reader. Bottom: how the reader runs motion-aware phase control across the APP, MAC, and PHY layers. (b) Conceptual timing: a posture change leaves a residual carrier with a fixed phase, whereas updating the compensation phase θ_c in the next frame removes it.

bandwidth of the twin meander coil for NFC VHBR, but at such high bit rates the bridge becomes sensitive to any mismatch between the two coils. Knitted wiring stretches, so its impedance changes whenever the clothing bends, as is known for elastic and deformable coils and tags [17], [18], and the bridge loses its balance. We solve this with motion-aware phase control, in which a digital bridge shifts only the phase between the two drive signals (Fig. 1(b)). This keeps the BER low for mismatch errors up to 70%, as when one arm is fully bent. As a proof of concept, we estimate the coil impedance by motion tracking and update the phase each time the TDMA time slot switches.

II. Digitally-Balanced Twin Meander Coil

A. System Configuration

Fig. 2(a) shows picoWear: the twin-meander-coil clothing connected to the reader module, and an on-skin tag. Two meander coils, with impedances Z_1 and Z_2, cover the left and right halves of the body. Splitting the meander into twin coils widens the bandwidth to about $13.56\,\mathrm{MHz} \pm 3\,\mathrm{MHz}$ (10.5–16.5 MHz), which passes the sidebands of the $1.7\,\mathrm{Mbit/s}$ link. The meander coils are knitted from conductive yarn (AgFit) on a WHOLEGARMENT knitting machine (MACH15S, Shima Seiki), with a line width of $13\,\mathrm{mm}$ and a gap of $50\,\mathrm{mm}$ between lines, the same as in the simulation. Each coil is tuned to $13.56\,\mathrm{MHz}$ with distributed series capacitors. We simulated picoWear on a human body model (Gustav, scaled to $170\,\mathrm{cm}$, with tissue properties at $13.56\,\mathrm{MHz}$) with the frequency-domain solver of CST Studio Suite. The lines are $0.5\,\mathrm{mm}$-thick conductors 7–$10\,\mathrm{mm}$ from the skin, and the capacitors are lumped elements; the conductivity and the line positions were set so that the inductance L and resistance R of each coil match those of the knitted prototype ($\sigma = 2.7 \times 10^4\,\mathrm{S/m}$). At $13.56\,\mathrm{MHz}$, $|H|$ falls by about $10\,\mathrm{dB}$ from $5\,\mathrm{mm}$ to $50\,\mathrm{mm}$ away from the clothing, midway between adjacent lines (Fig. 1(a)).

B. Operating Principle

Two sources drive the coils, and the currents returning from the two coils add up at the input of a transimpedance amplifier (Fig. 1(b)). This cancellation works like self-interference cancellation in full-duplex receivers. The receiver therefore sees

$$V_{\mathrm{out}} = -R_{\mathrm{f}} I_{\mathrm{out}} = -R_{\mathrm{f}} \left(\frac{V_1}{Z_1} + \frac{V_2}{Z_2} \right), \tag{1}$$

where V_1 and V_2 are the drive voltages, Z_1 and Z_2 are the coil impedances, I_{out} is the summed current, and R_{f} is the feedback resistance. The carrier disappears ($V_{\mathrm{out}} = 0$) when

$$V_1 = -\frac{Z_1}{Z_2} V_2. \tag{2}$$

In this state, the receiver sees only the small change caused by the tag, so it can use a high gain without saturating.

A conventional twin meander coil drives the two coils in antiphase, $V_1 = -V_2$, which cancels the carrier when $Z_1 = Z_2$. Unfortunately, when the wearer moves, the two coils bend differently, and the tag also changes Z_1. With (1), the output becomes, to first order,

$$V_{\mathrm{out}} \approx \frac{R_{\mathrm{f}} \left(\Delta Z_1 + \Delta Z_{\mathrm{tag}} \right)}{Z^2} V_1, \tag{3}$$

where Z is the balanced coil impedance ($Z_1 = Z_2 = Z$), and ΔZ_1 and ΔZ_{tag} are the changes in Z_1 caused by bending and by the tag. The ΔZ_{tag} term is the tag signal, and the ΔZ_1 term is a leftover carrier. We call $|\Delta Z_1|/|Z|$ the mismatch error. This leftover carrier adds to the tag signal and makes the *0* and *1* symbols harder to tell apart (fixed-phase trace in Fig. 2(b)). Even during ordinary movements, the mismatch error often exceeds 50%, and the $1.7\,\mathrm{Mbit/s}$ link fails without motion-aware phase control.

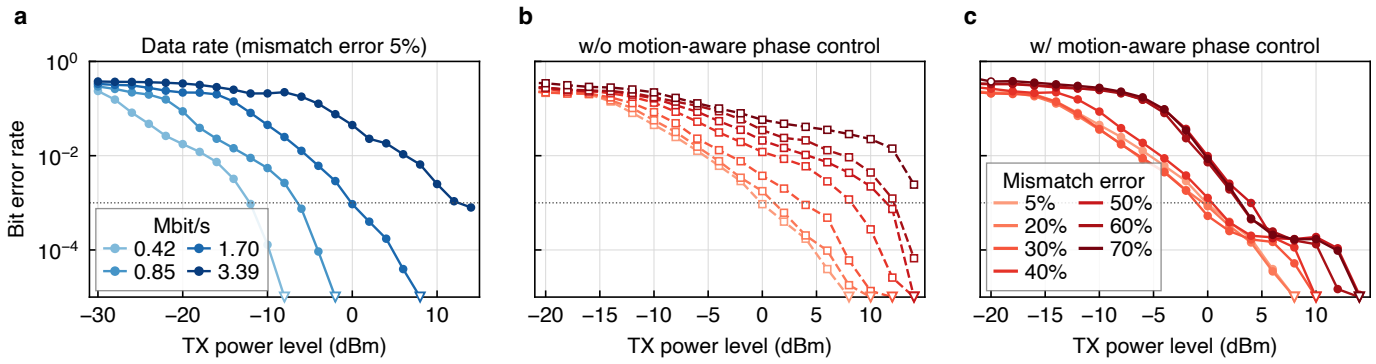


Fig. 3. BER of the tag-to-reader link. (a) Data rates at a mismatch error of 5%. (b) Mismatch errors of 5%–70% at 1.7 Mbit/s without and (c) with motion-aware phase control. Triangles: BER below 10^{-5}; open circles: fewer than 100 frames.

C. Digital Bridge

Because the drive signals are made digitally, (2) can be met for any Z_1 and Z_2. Ideally, the amplitude ratio of V_1 to V_2 is set to $|Z_1/Z_2|$, and their phase difference, which we call the compensation phase θ_c, to $\pi + \angle(Z_1/Z_2)$. This removes the leftover carrier (trace with phase control in Fig. 2(b)). For a small mismatch, we write $Z_1/Z_2 = 1 + \delta$ with $|\delta| \ll 1$. The amplitude ratio is then about $1 + \mathrm{Re}(\delta)$, and the phase shift about $\mathrm{Im}(\delta)$ rad. In picoWear, bending mainly changes the reactance of the coils, from about $-22\,\Omega$ to $0\,\Omega$, whereas the resistance varies by only 1–2 Ω (standard deviation; Section IV). The phase term therefore dominates, and shifting the phase of one drive signal is enough for the bending we tested. In all experiments, only θ_c is changed. Section III confirms this by measurement.

III. Bit Error Rate Evaluation

A. Setup

We measured the BER of the link from the tag to the reader. First, we compared four bit rates, $f_c/32$, $f_c/16$, $f_c/8$, and $f_c/4$ (0.42, 0.85, 1.70, and 3.39 Mbit/s), where $f_c = 13.56$ MHz, to find the highest rate that works at a TX power level of 10 dBm. We then studied the effect of the mismatch error at $f_c/8$, the VHBR rate. Two USB instruments with signal generators and oscilloscopes (ADP3250, Digilent) ran the test. One made the data signal for the tag. The other made the two drive signals V_1 and V_2, which reached the coils through the digital-bridge board, and recorded the received signal. RF transformers isolate the tag and reader grounds from the instruments, as on a wearer. The tag is a coil tuned to 13.56 MHz with an RF switch (MASWSS0179, MACOM) that shorts the coil according to the data. It sends BPSK frames, each with a preamble, a Barker-13 sync word, and a 600-bit PRBS9 payload, without error correction. A PC demodulated the recorded signal by AM demodulation, as in the receiver of a commercial NFC reader IC (ST25R3911, STMicroelectronics). Even when the wearer bends one arm as far as possible, the mismatch error reaches only about 70%, so we measured the BER for mismatch errors of up to 70%, set by bending the arm. For each point, we counted at least 100 errors in at least 6×10^5 bits, or sent 10^7 bits. The TX power level is the output of each generator channel; 10 dBm equals 1 V peak into 50 Ω, not the power delivered to the coils. Without motion-aware phase control, the phase difference was fixed at 180°. With motion-aware phase control, it was set from the impedance ratio, which gave 184–213° for mismatch errors of 20%–70%.

B. Results

Fig. 3(a) shows the BER at each bit rate. The BER reaches 10^{-3} at −12.1, −6.5, and −0.1 dBm for 0.42, 0.85, and 1.70 Mbit/s. Each doubling of the bit rate costs about 6 dB. At 3.39 Mbit/s, 12.5 dBm is needed, probably because the meander coils have a limited bandwidth; at 10 dBm, $f_c/8$ is therefore the limit. We therefore use 1.7 Mbit/s from here on.

Fig. 3(b) and (c) show the BER at 1.7 Mbit/s without and with motion-aware phase control. Without it, the curves move to higher TX power levels as the mismatch error grows. At 70%, the BER does not reach 10^{-3} even at 14 dBm. With motion-aware phase control, all curves move back close to the balanced case. The required TX power level drops by 7.8, 7.5, and 9.2 dB at 40%, 50%, and 60%, and by more than 11 dB at 70%. In all cases, it stays within 4.1 dB of the level at 5%. Above 40%, these curves level off at a BER of 1–2×10^{-4} between 4 and 10 dBm. This floor is consistent with the remaining amplitude mismatch, which amplitude control could also remove. Shifting the phase of the drive signals is thus enough to keep the 1.7 Mbit/s link working when the clothing deforms.

IV. Communication During Motion

To run motion-aware phase control while the wearer moves, the reader needs Z_1/Z_2. An impedance analyzer cannot measure it during communication, as it stops the carrier to send its own test signal. We therefore estimate it from the shape of the clothing. We track seven points on the clothing (two on each sleeve and three on the shoulders and neck) with an optical motion-capture system (OptiTrack Flex 3, NaturalPoint); small inertial sensors (IMUs) will replace it in a final system. An ExtraTrees model, trained on impedances measured with a network analyzer (NanoVNA-H4, Hugen) during 4 min of free movement, maps these positions to the coil impedances. On 9464 test frames held out in 20 time blocks, it estimates the

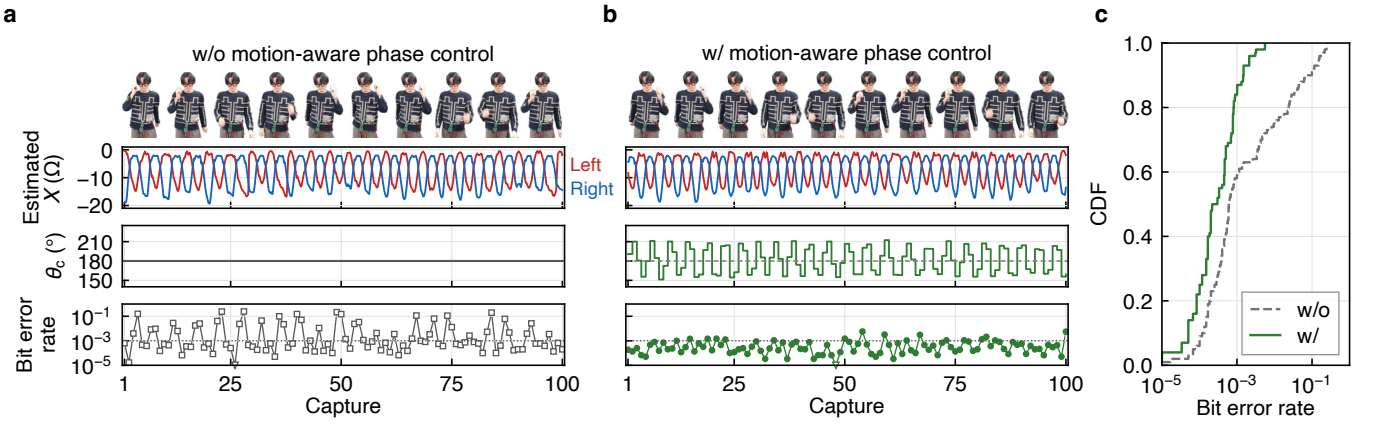


Fig. 4. BER at 1.7 Mbit/s and a TX power level of 10 dBm while the wearer moves (one point per 0.05 s capture, one every 0.7–0.8 s; triangles: no error). (a) Fixed phase and (b) motion-aware phase control: the wearer (one frame every 0.33 s), estimated reactance, phase, and BER. (c) CDF of the BER for captures matched in mismatch error.

reactance of the left and right coils with R^2 of 0.97 and 0.95 (RMS error 0.95 and 1.2 Ω).

We ran two 2 min sessions of free movement, without and with control, both at 1.7 Mbit/s and a TX power level of 10 dBm, one tenth of the 20 dBm typical of NFC readers. Fig. 4 shows the first 100 captures of each from 20 s; a capture lasts 0.05 s, and one starts every 0.7–0.8 s, so the link is sampled, not run without a break. After each capture, the reader set the phase for the next one from the estimated impedances. When the wearer raises an arm, the estimated reactance of that coil falls to about −18 Ω, and the phase follows (Fig. 4(b)). The BER fell from 2.1×10^{-2} with the phase fixed at 180° to 6.0×10^{-4} overall, and to 6.1×10^{-4} when each capture without control is paired with the capture with control of the closest estimated mismatch error (100 pairs, median gap 0.2%; Fig. 4(c)); the share of captures above 10^{-3} fell from 41% to 16%. The remaining errors arise as the phase lags fast motion and the estimate is off by about 1 Ω.

V. Conclusion

We have shown picoWear, meander-coil clothing that keeps a 1.7 Mbit/s NFC link while the wearer moves. A digital bridge balances the two coils by shifting only the phase between the two drive signals. This alone cut the TX power level needed for a BER of 10^{-3} by more than 11 dB when one arm is fully bent (70% mismatch error). Changing the phase with the wearer's motion lowered the BER during free movement from 2.1×10^{-2} to 6.1×10^{-4}. Next, we will predict the coil impedance 0.1 s ahead from IMUs on the tags. An FPGA-based NFC VHBR reader is designed to switch the phase in 0.1 ms (ADP3250: 5 ms) and update it every 10 ms.

References

[1] T. Yokota *et al.*, "A conformable imager for biometric authentication and vital sign measurement," *Nature Electronics*, vol. 3, no. 2, pp. 113–121, 2020.

[2] H. Hu *et al.*, "A wearable cardiac ultrasound imager," *Nature*, vol. 613, no. 7945, pp. 667–675, 2023.

[3] Y. Jiang, K. Pan, T. Leng, and Z. Hu, "Smart textile integrated wireless powered near field communication body temperature and sweat sensing system," *IEEE J. Electromagn., RF Microw. Med. Biol.*, vol. 4, no. 3, pp. 164–170, 2020.

[4] R. Lin, H.-J. Kim, S. Achavananthadith, and J. S. Ho, "Digitally-embroidered liquid metal textiles for near-field wireless body sensor networks," in *Proc. IEEE 17th Int. Conf. Wearable Implantable Body Sensor Netw. (BSN)*, 2021, pp. 1–4.

[5] W. Xu, T. Li, Y. Wang, X.-D. Yang, and T.-Y. Wu, "BIT: Battery-free, IC-less and wireless smart textile interface and sensing system," in *Proc. CHI Conf. Human Factors Comput. Syst.*, 2025, pp. 1–18.

[6] R. Takahashi, W. Yukita, T. Sasatani, T. Yokota, T. Someya, and Y. Kawahara, "Twin meander coil: Sensitive readout of battery-free on-body wireless sensors using body-scale meander coils," *Proc. ACM Interact. Mob. Wearable Ubiquitous Technol.*, vol. 5, no. 4, pp. 1–21, 2021.

[7] R. Takahashi, W. Yukita, T. Yokota, T. Someya, and Y. Kawahara, "Meander coil++: A body-scale wireless power transmission using safe-to-body and energy-efficient transmitter coil," in *Proc. CHI Conf. Human Factors Comput. Syst.*, 2022, pp. 1–12.

[8] M. S. Mohammadi, E. Dutkiewicz, Q. Zhang, and X. Huang, "Optimal energy efficiency link adaptation in IEEE 802.15.6 IR-UWB body area networks," *IEEE Commun. Lett.*, vol. 18, no. 12, pp. 2193–2196, 2014.

[9] C. Gong, X. Luo, Y. Xu, L. Li, and H. Liu, "A wearable ISM-band near-field antenna for data secure in metamaterial-textile-based WBANs," *IEEE Trans. Antennas Propag.*, vol. 74, no. 5, pp. 4819–4823, 2026.

[10] P. S. Hall, Y. Hao, Y. I. Nechayev *et al.*, "Antennas and propagation for on-body communication systems," *IEEE Antennas Propag. Mag.*, vol. 49, no. 3, pp. 41–58, 2007.

[11] J. Li, Y. Dong, J. H. Park, and J. Yoo, "Body-coupled power transmission and energy harvesting," *Nature Electronics*, vol. 4, no. 7, pp. 530–538, 2021.

[12] M. Abdolrazzaghi, R. Genov, and G. V. Eleftheriades, "High-efficiency inductive powering and auto-localization of CMOS brain implants by a wearable metasurface and coupled matching," *IEEE Microw. Wireless Technol. Lett.*, vol. 36, no. 6, pp. 962–965, 2026.

[13] M. Wagih, A. Komolafe, A. S. Weddell, and S. Beeby, "Broadband compact substrate-independent textile wearable antenna for simultaneous near- and far-field wireless power transmission," *IEEE Open J. Antennas Propag.*, vol. 3, pp. 398–411, 2022.

[14] R. Takahashi, C. Han, W. Yukita, J. S. Ho, T. Sasatani, A. Noda, T. Yokota, T. Someya, and Y. Kawahara, "Full-body NFC: Body-scale near-field sensor networks with machine-knittable meandered e-textiles," arXiv:2503.13240, 2025.

[15] R. Maeda and A. Noda, "Protocol-flexible custom NFC for wire-free wearable sensor networks," *IEEE Sens. Lett.*, vol. 10, no. 11, p. 5506104, 2026.

[16] B. Couraud, R. Vauche, T. Deleruyelle, and E. Kussener, "A very high bit rate test platform for ISO 14443 and interoperability tests," in *Proc. IEEE 16th Int. Conf. Commun. Technol. (ICCT)*, 2015, pp. 353–356.

[17] B. Kahraman-Agir, K. Yegin, and E. Ozturk-Isik, "Wearable and elastic surface coil for ^{1}H magnetic resonance imaging," *IEEE Microw. Wireless Compon. Lett.*, vol. 31, no. 5, pp. 517–520, 2021.

[18] Y. Chen, T. Lv, J. Lu, and Y. Yang, "Deformation-resistant broadband RFID tag for multidielectric-platform environments," *IEEE Microw. Wireless Technol. Lett.*, 2025, early access.